Nuclear Physics B349 (1991) 109–131
North-Holland

RADIATIVE CORRECTIONS TO CHARGED-CURRENT DEEP INELASTIC SCATTERING AT HERA

H. SPIESBERGER*

II. Institut für Theoretische Physik der Universität Hamburg, Luruper Chaussee 149, 2000 Hamburg 50, Germany

Received 14 May 1990
(Revised 27 August 1990)

The complete $O(\alpha)$ electromagnetic and weak radiative corrections for the differential cross section $d^2\sigma/dx\,dy$ of the charged-current deep inelastic lepton–proton scattering at HERA are calculated. A Monte Carlo integration technique for the evaluation of the single photon bremsstrahlung contribution is explained. We derive formulas that are relevant for the exponentiation of soft photonic corrections and show numerical results. Those differences in the predictions are discussed that arise when either M_W or the μ decay constant G_μ is used as input. In particular the top quark mass dependence of the NC/CC cross section ratio is investigated.

1. Introduction

Radiative corrections for deep inelastic lepton–proton scattering at HERA have been calculated in the past by two independent groups (Bardin et al. [1,2] and Böhm and Spiesberger [3,4]). Recently a comparison of the results has led to the conclusion that the $O(\alpha)$ corrections for the neutral current cross section are sufficiently well understood [5,6]. The leptonic corrections to the charged current process have been calculated in the leading logarithmic approximation in ref. [7]. But a confirmation of the results for the complete $O(\alpha)$ electroweak corrections for charged current scattering is still missing. In ref. [2], the electroweak corrections for CC scattering have been presented, the calculations following the same lines as for the NC process [1], whereas in ref. [4] the full corrections had been given only for the partially integrated cross section $d\sigma/dQ^2$.

In this note we present results for the charged current twofold differential cross section $d^2\sigma/dx\,dy$ that confirm those of ref. [2]. The calculation of the bremsstrahlung contributions is performed using a Monte Carlo integration technique which will prove valuable in a future development of a Monte Carlo event

*Supported by Bundesministerium für Forschung und Technologie, 05 4HH 92P/3, Bonn, Germany.

generator for the simulation of charged current events including radiative effects [8]. We shall explain the method in some detail.

The corrections are known to grow large but negative in the low y–high x region. This behavior is due to the dominance of soft photon corrections. It is well known that for an adequate description of this situation higher order corrections are needed. These may be derived from the exponentiation prescription à la Yennie et al. [9]. We have derived the relevant formulas and present numerical results for the corrections including multiple photon effects.

Through the self-energy corrections the deep inelastic cross sections depend on the yet unknown masses of the top quark and the Higgs boson. We shall discuss the question whether the measurement of the ratio of neutral current over charged current cross sections $R_\pm$ for electron or positron scattering could be used to derive limits on the top quark mass. The sensitivity of $R_\pm$ on m_t depends on the choice of the input parameters: the theory can be fixed either by the weak boson masses M_Z and M_W or by M_Z and the μ decay constant G_μ. In the latter case, M_W must be calculated from G_μ by a formula that includes $O(\alpha)$ corrections, too. The resulting value for M_W (and consequently the coupling constants via $s_W^2 = 1 - M_W^2/M_Z^2$) also receive an m_t dependence. In the case where G_μ is used, the final top mass dependence is rather flat and a derivation of m_t limits from $R_\pm$ would require high precision measurements. One does not gain much in using a fixed value for M_W as input. Although the sensitivity of $R_\pm$ on m_t is increased thereby, the experimental uncertainty on the value of the W boson mass will probably not allow us to derive statements on the value of m_t.

2. The non-radiative cross section

We start by repeating some basic formulas for the Born cross section. The kinematical variables Q^2, x, and y are determined by

$$Q^2 = -(p-p')^2, \qquad x = \frac{Q^2}{2P(p-p')},$$

$$y = \frac{P(p-p')}{Pp} = \frac{Q^2}{xS} \tag{1}$$

from the 4-momenta p, p', and P of the incoming charged lepton, the outgoing neutrino and the proton. S is the square of the center-of-mass energy $S = (p+P)^2$. The neutrino momentum p' cannot be measured directly, but we assume that it can be reconstructed from the measurement of the hadronic final state [10]. The determination of x and Q^2 from measured momenta will deserve further comments if there is an additional photon (see below).

The lowest order cross section reads

$$\left.\frac{\mathrm{d}^2\sigma}{\mathrm{d}x\,\mathrm{d}y}\right|_{\mathrm{CC}}^{\mathrm{Born}} = \frac{\pi\alpha^2}{2s_{\mathrm{W}}^4}\frac{xS}{\left(Q^2+M_{\mathrm{W}}^2\right)^2}\left\{q+(1-y)^2\bar{q}\right\}. \tag{2}$$

The parton distribution functions enter in the combinations

$$q=\begin{cases}u+c & \text{for } \mathrm{e}^- \\ d+s & \text{for } \mathrm{e}^+\end{cases} \quad \text{and} \quad \bar{q}=\begin{cases}\bar{d}+\bar{s} & \text{for } \mathrm{e}^- \\ \bar{u}+\bar{c} & \text{for } \mathrm{e}^+\end{cases}. \tag{3}$$

They are taken as input described by one of the parametrizations that are available in the literature. By their Q^2 dependence, QCD corrections in the leading logarithmic approximation are taken into account. Radiative corrections of QCD origin are, however, not discussed in this paper. We restrict ourselves to the study of electroweak effects.

The Feynman diagrams describing the virtual $O(\alpha)$ electroweak corrections are shown in fig. 1. The relevant formulas have been given in ref. [4] (see also ref. [11]) and lead to an overall correction $1+\delta_{\mathrm{CC}}^{\text{1-loop}}$ to the cross section. The basic building blocks needed for the calculation of $\delta_{\mathrm{CC}}^{\text{1-loop}}$ are self-energies, vertex corrections, and box diagrams [12]. They were calculated in the on-mass-shell renormalization scheme (OMS). In this renormalization scheme, the basic parameters in the formulation of the lagrangian and the counterterms are the fine structure constant α, the weak boson masses $M_{\mathrm{W}}, M_{\mathrm{Z}}$, the Higgs mass M_{H}, and the fermion masses m_{f}. The conditions that fix the counterterms express the requirement that the mass parameters describe the experimentally observable positions of the poles of the respective propagators. Each physical observable is determined as a function of these basic parameters.

A drawback of this scheme is the fact that the W boson mass M_{W} is not yet well measured directly. It has therefore become customary to use as experimental input instead of M_{W} the measurement of the μ decay constant G_μ. The formulation of the theory and the definition of counterterms is thereby not affected: M_{W} still describes the physical W mass. The on-mass-shell scheme where this experimental input is used is sometimes called the modified on-mass-shell scheme (MOMS). In lowest order the relation

$$G_\mu = \frac{\pi\alpha}{\sqrt{2}}\frac{1}{s_{\mathrm{W}}^2 M_{\mathrm{W}}^2} \tag{4}$$

describes the transformation from one scheme to the other. In order to be consistent one has to include radiative corrections to μ decay in this relation, too, when calculating predictions for other observables in higher orders. Higher order corrections to eq. (4) are traditionally collected into a factor $1-\Delta r$ [13] changing

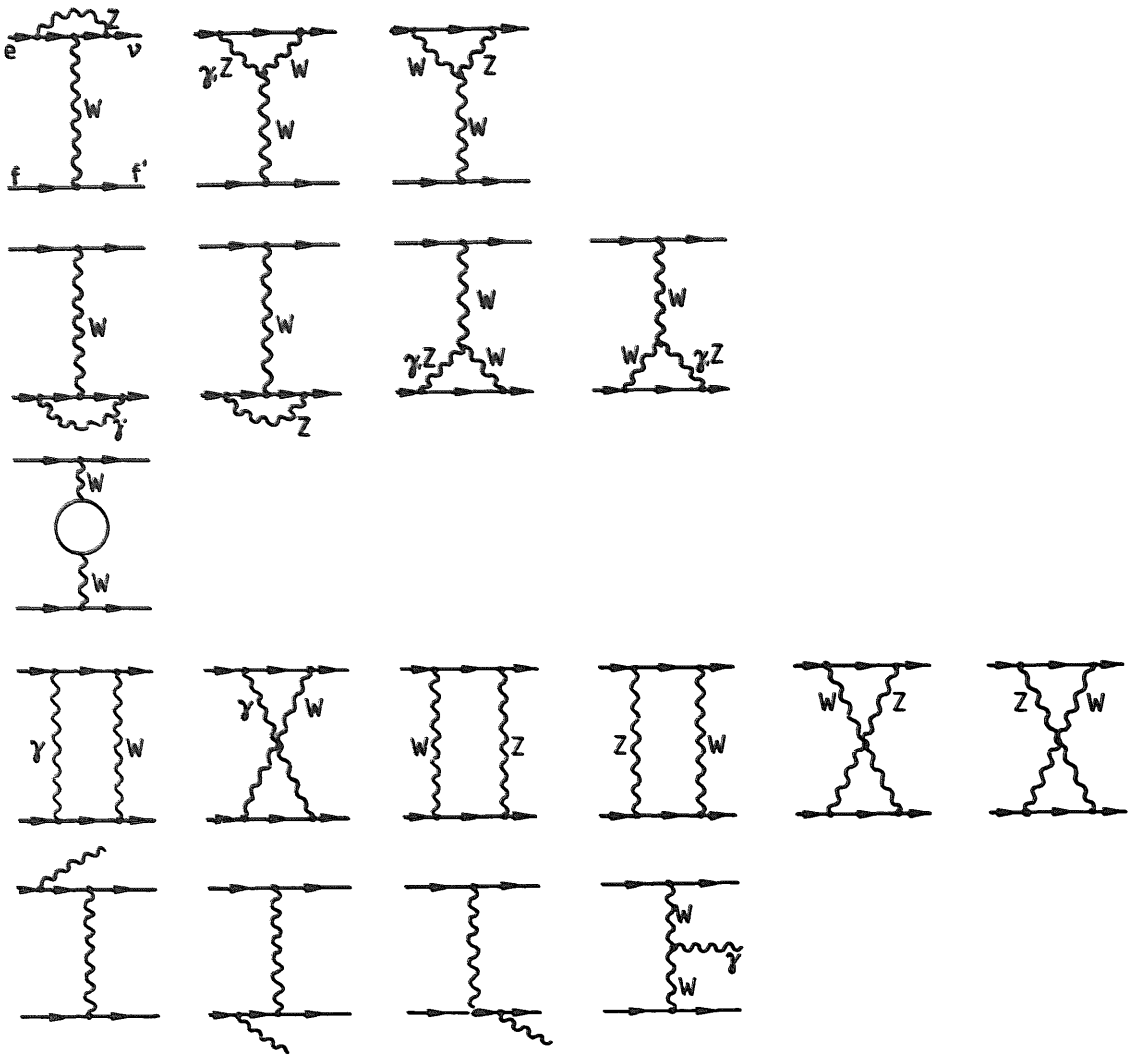

Fig. 1. Feynman diagrams contributing to the O(α) radiative corrections for charged current scattering.

eq. (4) into

$$G_\mu = \frac{\pi\alpha}{\sqrt{2}} \frac{1}{s_W^2 M_W^2} \frac{1}{1-\Delta r}. \tag{5}$$

We shall discuss the consequences of using G_μ as experimental input instead of a fixed value for M_W in some more detail below.

The photonic part of $\delta_{CC}^{1\text{-loop}}$ contains infrared divergent contributions. To deal with them, the emission of real photons must also be considered. The bremsstrahlung cross section is split into a soft part, where the emission of a photon up to a maximal energy k_0 is included and a hard part where the photon energy is bigger than k_0. The soft part is treated analytically in the soft photon approximation and results in a correction δ_{CC}^{soft}. The infrared divergence is con-

tained in this part and cancels against that coming from virtual photonic corrections: $\delta_{CC}^{soft} + \delta_{CC}^{1\text{-loop}}$ is infrared finite but depends on the unphysical parameter k_0. The dependence on k_0 will disappear when hard photons are included. In the numerical evaluation the cutoff k_0 is chosen to be small as compared to the energies of the fermions such that the soft photon approximation is justified. k_0 is also chosen smaller than the experimental resolution for photon detection. The soft bremsstrahlung thus describes the emission of unobserved photons and contributes to the non-radiative cross section

$$\left.\frac{d^2\sigma}{dx\,dy}\right|_{CC}^{nr} = \left(1 + \delta_{CC}^{1\text{-loop}} + \delta_{CC}^{soft}\right)\left.\frac{d^2\sigma}{dx\,dy}\right|_{CC}^{Born}. \tag{6}$$

In the neutral current process there is a direct way of classifying the corrections into purely electromagnetic and purely weak ones. The electromagnetic contributions can be further separated into parts describing leptonic radiation, radiation from the quark line and the interference of leptonic and quarkonic radiation. Such a classification is not only helpful for a better understanding of general features of the corrections. It is also necessary for the separation of the quarkonic corrections. These contain mass singularities $\propto \ln(m_f^2/Q^2)$ which have to be factorized and absorbed into the definition of the quark distribution functions [14]. Otherwise the predictions for the deep inelastic cross sections would depend on ill-defined quark masses.

The appearance of diagrams with the non-abelian WWγ coupling prevents us from seeing immediately how the corrections could be separated into leptonic, quarkonic, and lepton–quark interference parts. This separation is obviously not possible in terms of Feynman diagrams. In ref. [2] it has been shown how it can be derived nevertheless in a gauge invariant way. For this one has to express the charge of the outgoing quark with flavor f', $Q_{f'}$, and of the W boson, Q_W, by the charges of the initial quark with flavor f, Q_f, and the lepton, Q_ℓ, by

$$|Q_\ell| = |Q_W|, \qquad Q_{f'} = Q_\ell + Q_f. \tag{7}$$

The different terms in the bremsstrahlung cross section [4] can then be rearranged into the form

$$\left.\frac{d^2\sigma}{dx\,dy}\right|_{CC}^{BS} = \left(Q_\ell^2 L(x,y) + Q_\ell Q_f I(x,y) + Q_f^2 H(x,y)\right). \tag{8}$$

In the same way the virtual and soft corrections are separated into a leptonic, an interference, and a hadronic part. The mass singularities due to the incoming lepton are then all contained in L, those of the incoming quark in H. They can be

calculated explicitly, e.g. in the collinear approximation and it can be shown that the singular terms are process independent. Thus the basic assumption of the parton model is not upset: deep inelastic processes can be described by cross sections that factorize into process-independent quark distribution functions and singularity free cross sections for hard subprocesses.

There are also mass singularities from the final quark $\simeq \ln(m_f^2/Q^2)$ in individual terms contributing to L, I, and H, but as is expressed in the Kinoshita–Lee–Nauenberg theorem these mass logarithms will cancel whence virtual and soft parts are combined with the corresponding hard photonic contributions. The independence of the final results on m_f provides a check of the correctness of the numerical results.

3. Single photon bremsstrahlung

In this section we discuss the contribution from hard bremsstrahlung. Some of the emitted photons in this case can have energies above the detection threshold. But even if their energy would be large enough for detection they need not be observable in a realistic experiment. Most of them will disappear down the beam pipe faking a non-radiative event. The calculation of the cross section for events of this type would need the introduction of cuts in the angle variables. But instead of complicating the calculation by this we prefer to perform the phase space integration without any restriction. The assignment of 4-momenta to the incoming and outgoing particles that we use to describe the radiative lepton–quark scattering $eq \to \nu q'\gamma$ are shown in fig. 2. We shall also use the invariants for the lepton–quark

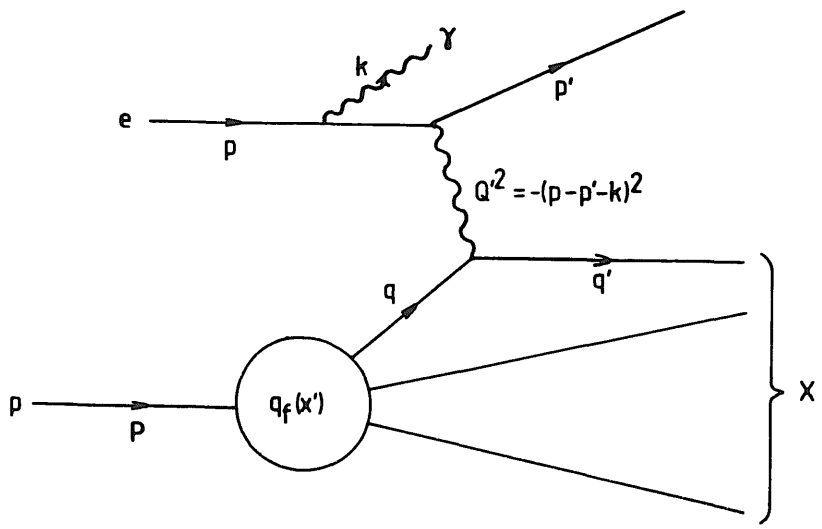

Fig. 2. Notations for the bremsstrahlung in the lepton–quark scattering.

subprocess

$$s=(p+q)^2=x'S, \qquad t=(p-p')^2=-xyS, \qquad u=(p'-q)^2=-x'(1-y)S. \tag{9}$$

The phase space integration is performed in the reference frame where $k+q'=0$. The transformation from the HERA laboratory reference frame to this "center-of-mass" system depends on the energy of the incoming quark which is described by the variable x'. The energies in this frame are given by

$$E_q=\frac{x'yS-m_e^2}{2E_{tot}}, \qquad E_e=\frac{(x'-xy)S-m_f^2}{2E_{tot}},$$

$$E_\nu=\frac{(xy+x'(1-y))S+m_e^2+m_f^2}{2E_{tot}}, \qquad E_\gamma=\frac{(x'-x)yS-M^2}{2E_{tot}},$$

$$E_{q'}=E_e+E_q-E_\nu-E_\gamma=\sqrt{E_\gamma^2+m_{f'}^2},$$

$$E_{tot}=E_e+E_q-E_\nu=\sqrt{(x'-x)yS-m_e^2-m_f^2}, \tag{10}$$

where $M^2=m_e^2+m_f^2+m_{f'}^2$ is the sum of the squares of all involved fermions.

The advantage in using this reference frame lies in the fact that the phase space is independent of angle variables. Including the averaging over the initial state which is parametrized by x' it reads

$$\int dx' \int \frac{d^3p'}{2E_\nu}\frac{d^3q'}{2E_{q'}}\frac{d^3k}{2E_\gamma}\delta^4(p+q-p'-q'-k)=\frac{\pi yS}{8}\int dx\,dy\int dx'\frac{E_\gamma}{E_{tot}}\,dz\,d\phi. \tag{11}$$

The integration over the photon energy has been performed using the δ function for the energy–momentum conservation. $z=\cos\theta$ and θ and ϕ are polar and azimuthal angle of the photon with respect to some appropriately chosen axis.

The lower limit of the x' integration, x'_{min}, is determined from the minimally allowed photon energy k_0. We decided to define k_0 in the HERA laboratory reference frame. This will be advantageous in the development of a Monte Carlo event generator. Although k_0 is an unphysical parameter, it can then be used to define an experimental minimum of the photon energy such that soft photons can

be effectively cut out. Therefore we have to solve

$$E^{\mathrm{H}}_{\gamma,\max}(x,y;x'_{\min}) = k_0\,, \tag{12}$$

where $E^{\mathrm{H}}_{\gamma,\max}(x,y;x')$ is the maximum of the photon energy with respect to the emission angle in the HERA lab-system for fixed x'. It is given by

$$E^{\mathrm{H}}_{\gamma,\max}(x,y;x') = \frac{s+t+u-M^2}{s+t+u-M^2+m_{\mathrm{f}}^2} \times\left\{E^{\mathrm{H}}_{\mathrm{e}}+E^{\mathrm{H}}_{\mathrm{q}}-E^{\mathrm{H}}_{\nu}+\sqrt{\left(|\boldsymbol{p}^{\mathrm{H}}_{\mathrm{e}}|-|\boldsymbol{q}^{\mathrm{H}}|-|\boldsymbol{p}^{\mathrm{H}}_{\nu}|\cos\theta^{\mathrm{H}}_{\nu}\right)^2+|\boldsymbol{p}^{\mathrm{H}}_{\nu}|^2\sin^2\theta^{\mathrm{H}}_{\nu}}\right\}, \tag{13}$$

where all energies, momenta, and the neutrino scattering angle θ_ν are taken in the HERA reference frame. The solution of eq. (12) for $k_0 = 0$ is $x'_{\min}(0) = x + M^2/yS$. For small $k_0/E^{\mathrm{H}}_{\mathrm{e}}$ it is

$$x'_{\min} = x + \frac{M^2}{yS} + \frac{k_0}{E^{\mathrm{H}}_{\mathrm{e}}}\frac{m_{\mathrm{f}}^2}{yS}\frac{1}{y+x(1-y)\sigma}\,, \tag{14}$$

where $\sigma = E^{\mathrm{H}}_{\mathrm{proton}}/E^{\mathrm{H}}_{\mathrm{e}}$ is the ratio of the proton and the electron energies. Note that for fixed $x' > x + M^2/yS$ the emission of zero-energy photons is kinematically not allowed. Only for elastic scattering without emission of energy by an additional photon is the Bjorken identification $x' = x$ derived (up to terms of order $O(m_{\mathrm{f}}^2)$).

The infrared divergence appears at the lower limit of the x' integration as the limit $E_\gamma \to 0$ corresponds to $x' \to x + M^2/yS$. After substituting for the variable

$$u = \log(x' - x - M^2/yS)\,,$$

the x' integration is completely well behaved.

We want to add a further comment on the angular integration. Whereas the ϕ integration does not lead to difficulties, one cannot use directly the polar angle θ because of the strong peaking behavior of the differential cross section in the directions of the charged fermions. This angular dependence is determined by the factors

$$\frac{1}{kp_i} = \frac{1}{E_\gamma(E_i - |\boldsymbol{p}_i|\cos\theta)} \tag{15}$$

appearing in the modulus squared of the bremsstrahlung matrix element. Instead

of using θ one transforms to the variable

$$v_i = \log(1 - (|\boldsymbol{p}_i|/E_i)\cos\theta).$$

This substitution results in a flat v_i dependence. It is performed for the terms $\simeq 1/kp$ (leptonic radiation) and $\simeq 1/kq$ (quarkonic radiation) separately, choosing $\boldsymbol{p}$ and $\boldsymbol{q}$ as polar axis, respectively. In case of emission from the final quark (terms $\simeq 1/kq'$) this difficulty does not appear because of the choice of the reference frame where $\boldsymbol{k} + \boldsymbol{q}' = 0$ and the factor

$$\frac{E_\gamma}{E_{\text{tot}}}\frac{1}{kq'} = \frac{1}{E_{\text{tot}}^2}. \tag{16}$$

is independent of angle variables. Similarly, transformations can be found that render the double pole terms $\simeq m_i^2/(kp_i)^2$ harmless.

The fact that k_0 is defined independent of the photon emission angle in the HERA reference frame has the consequence that the integration limits for θ and ϕ in the "center-of-mass" system are not always trivial. This is the case if x' has a value such that

$$E_{\gamma,\min}^{\text{H}}(x, y; x') < k_0. \tag{17}$$

where $E_{\gamma,\min}^{\text{H}}$ is given by eq. (12) with the plus sign in front of the square root replaced by a minus sign. Above x'_{cut}, i.e. the value of x' where the inequality (17) becomes an equation, photons can be emitted into any direction and the limits of the angular integrations are simply $0 \leqslant \theta \leqslant \pi$ and $0 \leqslant \phi \leqslant 2\pi$. In the range $x'_{\min} \leqslant x' \leqslant x'_{\text{cut}}$ the limits for θ and ϕ have to be determined from

$$E_\gamma^{\text{H}} = \frac{|\boldsymbol{p}_{\text{e}}^{\text{H}}|kq + |\boldsymbol{q}^{\text{H}}|kp}{|\boldsymbol{p}_{\text{e}}^{\text{H}}|E_{\text{q}}^{\text{H}} + |\boldsymbol{q}^{\text{H}}|E_{\text{e}}^{\text{H}}} \geqslant k_0. \tag{18}$$

In the concrete calculation we have used x'_{cut} as a cut to separate the x' integration into two parts. By this, the amount of CPU time needed to reach a certain requested accuracy could be decreased. For the integration we used the general purpose Monte Carlo integration technique realized in the VEGAS routine [15].

The dependence of the sum of virtual, soft, and hard corrections on the IR cutoff k_0 is shown in fig. 3 for a selected point in the (x, y) plane. The result is independent of k_0 down to quite small values of k_0. Note that there is a strong cancellation between the soft and hard contributions. Individually they can be larger by an order of magnitude than the final result and depend strongly on k_0. The last two points in this figure for $k_0 = 0.063$ GeV and $k_0 = 0.126$ GeV lie

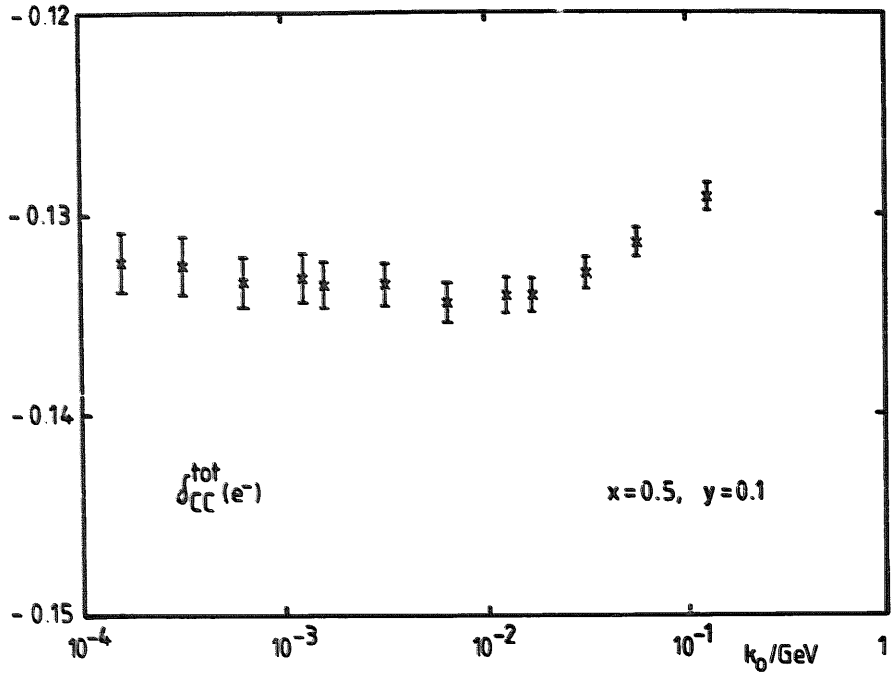

Fig. 3. The k_0 dependence of the complete O(α) radiative corrections ($x = 0.5$, $y = 0.1$).

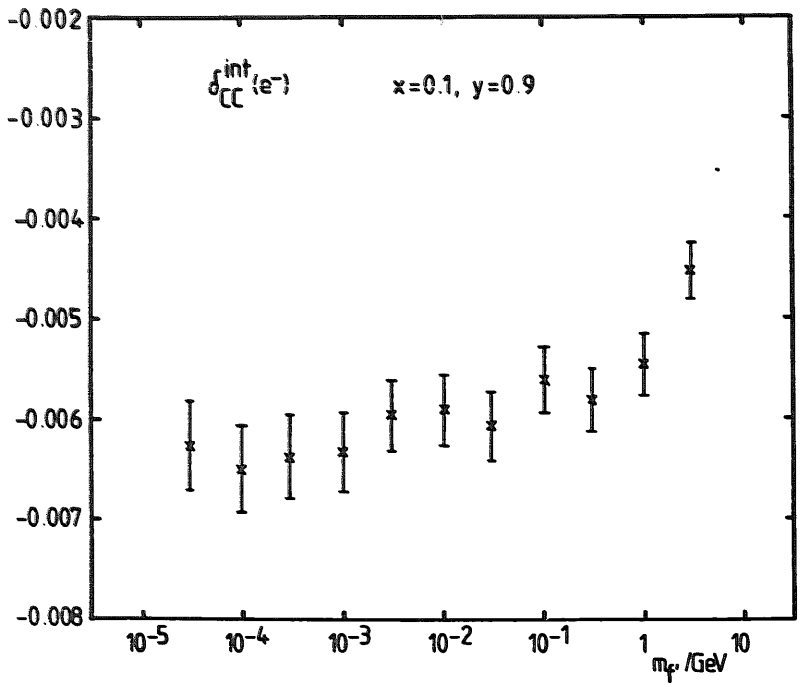

Fig. 4. The m_f dependence of the $\delta_{CC}^{mt}(e^-)$ ($x = 0.1$, $y = 0.9$).

somewhat above the results for smaller values of k_0 indicating that the soft photon approximation starts to fail. These values of k_0 correspond to 4 and 8% of $E^{H}_{\gamma,\min}(x, y; 1)$, i.e. the maximal value of the photon energy in the HERA laboratory system where the phase space is still isotropic (above $E^{H}_{\gamma,\min}(x, y; 1)$ photon emission is allowed only into a restricted range of angles). The error bars shown in this and the next figure are error estimates given by VEGAS after evaluation of 30,000 points. As a second check of the validity of our approach, fig. 4 shows the results for the lepton–quark interference part $\delta^{\text{int}}_{\text{CC}}(e^-)$ at $x = 0.1$, $y = 0.9$ for various values of the mass of the outgoing quark $m_{f'}$. The results are independent of $m_{f'}$ over a wide range of values. The smallest possible value for $m_{f'}$ where our program still works is only limited by the accuracy that is required in the determination of $x'_{\min}$ from eq. (12). Of course, large values of $m_{f'}$ constrain the phase space as is visible in the point for the largest value of $m_{f'}$ in fig. 4. $\delta^{\text{int}}_{\text{CC}}$ has the most complicated singularity structure as it contains all three collinear peaks. The results of figs. 3 and 4 are typical also for other values of x and y.

4. Exponentiation of soft photonic corrections

An inspection of eq. (13) for the maximally allowed energy of emitted photons shows that $E^{H}_{\gamma,\max}$ becomes small for $x \to 1$ and $y \to 0$. In the large x–small y region the soft photon corrections are thus dominating. They are numerically large and higher order contributions from multiple photons are expected to become important. Because one has to deal with a soft photon effect, it will be sufficient in this region of x and y to include in higher orders only these infrared photons and discard the infrared-finite corrections from hard photons [16].

Higher order corrections from soft photons have been discussed in the general case by Yennie et al. [9]. They have shown that the infrared divergences of both virtual and real corrections can be calculated recursively resulting in the exponential series. It is thus believed that the exponentiation of the remainder of virtual and real corrections after the cancellation of the divergent terms results in a better description of the true predictions of the theory. Explicit higher order calculations have confirmed this conjecture.

The calculation of those terms that are exponentiated is usually carried through in the soft photon approximation, separating out thereby certain infrared finite parts that are included only in their original nonexponentiated form. If the result of a complete $O(\alpha)$ calculation is a correction factor $1 + \delta^{\text{tot}} = 1 + \delta^{\text{1-loop}} + \delta^{\text{soft}} + \delta^{\text{hard}}$ one writes

$$1 + \delta^{\text{tot}} = 1 + \delta^{\text{IR}} + \delta^{\text{fin}} \to \exp\{\delta^{\text{IR}}\}(1 + \delta^{\text{fin}}). \tag{19}$$

A priori, the separation of photonic corrections into IR parts that should be exponentiated and non-IR, finite parts that are not exponentiated is arbitrary. One can always shift around non-IR contributions. But the separation of those parts that should be exponentiated is further restricted by the requirement that it should

be gauge invariant. Otherwise, the different prescriptions for the treatment of IR and non-IR pieces would lead to gauge-dependent predictions for physical observables. In addition to this, one imposes the requirement that the exponentiated terms should be ultraviolet finite. This means just a simplification of the calculation because the renormalization prescriptions that have been worked out in a finite order of perturbation theory remain unchanged.

The general form of the IR parts obeying these two additional conditions was given already in ref. [9]. In the following we present the explicit formulas as needed for the charged current reaction. The soft photonic parts are separated as discussed above into leptonic, quarkonic, and interference contributions. The sums of virtual and real IR corrections to the cross sections for scattering of leptons and quarks with flavor f read (in the notation of ref. [9])

$$2\alpha(\mathrm{Re}\,B+\tilde{B})_{\ell} = \frac{\alpha}{2\pi}\left\{\ln\frac{4K^2}{-u}\left(\ln\frac{-u}{m_e^2}+\ln\frac{-u}{m_{f'}^2}\right)-\ln\frac{K^2}{E_e^2}-\ln\frac{K^2}{E_{q'}^2}\right.$$
$$+\ln\frac{-u}{m_e^2}\left(\ln\frac{-u}{4E_e^2}+\frac{1}{2}\right)+\ln\frac{-u}{m_{f'}^2}\left(\ln\frac{-u}{4E_{q'}^2}+\frac{1}{2}\right)$$
$$\left.-\tfrac{1}{2}\ln^2\frac{-u}{4E_e^2}-\tfrac{1}{2}\ln^2\frac{-u}{4E_{q'}^2}-2\,\mathrm{Li}_2\left(1+\frac{4E_eE_{q'}}{u}\right)-\frac{\pi^2}{3}-2\right\}, \tag{20}$$

$$2\alpha(\mathrm{Re}\,B+\tilde{B})_q^{\mathrm{f}} = \frac{\alpha}{2\pi}Q_f^2\left\{\ln\frac{4K^2}{-t}\left(\ln\frac{-t}{m_f^2}+\ln\frac{-t}{m_{f'}^2}\right)-\ln\frac{K^2}{E_{q'}^2}-\ln\frac{K^2}{E_q^2}\right.$$
$$+\ln\frac{-t}{m_f^2}\left(\ln\frac{-t}{4E_q^2}+\frac{1}{2}\right)+\ln\frac{-t}{m_{f'}^2}\left(\ln\frac{-t}{4E_{q'}^2}+\frac{1}{2}\right)$$
$$\left.-\tfrac{1}{2}\ln^2\frac{-t}{4E_q^2}-\tfrac{1}{2}\ln^2\frac{-t}{4E_{q'}^2}-2\,\mathrm{Li}_2\left(1+\frac{4E_qE_{q'}}{t}\right)-\frac{\pi^2}{3}-2\right\}, \tag{21}$$

$$2\alpha(\mathrm{Re}\,B+\tilde{B})_i^{\mathrm{f}} = -\frac{\alpha}{2\pi}Q_{\ell}Q_f\left\{2\ln\frac{4K^2}{-u}\ln\frac{s}{-t}+2\ln\frac{K^2}{E_{q'}^2}+\ln\frac{-u}{m_{f'}^2}\left(2\ln\frac{E_{q'}^2}{K^2}-1\right)\right.$$
$$+2\,\mathrm{Li}_2\left(1+\frac{4E_qE_{q'}}{t}\right)+2\,\mathrm{Li}_2\left(1+\frac{4E_eE_{q'}}{u}\right)$$
$$-2\,\mathrm{Li}_2\left(1-\frac{4E_eE_q}{s}\right)+\ln^2\frac{-u}{4E_{q'}^2}$$
$$\left.+\ln^2\frac{t}{u}-\ln^2\frac{s}{-u}-\ln\frac{-t}{s}+\frac{4\pi^2}{3}+2\right\}. \tag{22}$$

In these equations K is the maximum of the photon energy and the soft bremsstrahlung cross section was integrated over all angles. If we want to treat the photon totally inclusive in the calculation of corrections to $\mathrm{d}^2\sigma/\mathrm{d}x\,\mathrm{d}y|_{\mathrm{CC}}$ we have to use these formulas in a reference frame where the upper limit of the phase space is isotropic, i.e. the maximal photon energy does not depend on angles. This is the case in the frame where $p + P - p' = 0$. In this frame the energies are given by eq. (10) with $x' = 1$ and

$$K = \tfrac{1}{2}\sqrt{y(1-x)S}\,. \tag{23}$$

The final prescription for the improved cross section is

$$\left.\frac{\mathrm{d}^2\sigma}{\mathrm{d}x\,\mathrm{d}y}\right|_{\mathrm{CC}}^{\mathrm{exp}} = \sum_{\mathrm{f}}(1+\delta^f_{\mathrm{fin}})\exp\{\delta^f_{\mathrm{YFS}}\}\left.\frac{\mathrm{d}^2\sigma}{\mathrm{d}x\,\mathrm{d}y}\right|^{\mathrm{Born}}_{\mathrm{eq_f}\to\nu\mathrm{q_f}} \tag{24}$$

where

$$\delta^f_{\mathrm{YFS}} = 2\alpha(\mathrm{Re}\,B+\tilde{B})_{\ell} + 2\alpha(\mathrm{Re}\,B+\tilde{B})^f_{\mathrm{q}} + 2\alpha(\mathrm{Re}\,B+\tilde{B})^f_{\mathrm{i}}\,. \tag{25}$$

$(\mathrm{d}^2\sigma/\mathrm{d}x\,\mathrm{d}y)|^{\mathrm{Born}}_{\mathrm{eq_f}\to\nu\mathrm{q_f}}$ are the Born cross sections for the quark subprocesses including the quark densities and δ^f_{fin} contains all other nonphotonic corrections and the IR-finite parts of the photonic corrections:

$$\delta^f_{\mathrm{fin}} = \delta^f_{\mathrm{tot}} - \delta^f_{\mathrm{YFS}}\,. \tag{26}$$

5. Numerical results

Numerical results for the electroweak radiative corrections to the charged-current deep inelastic scattering cross sections for incoming electrons as well as for positrons are shown in figs. 5–7. We show the quantities

$$\delta^a_{\mathrm{CC}}(e^{\pm}) = \left.\frac{\mathrm{d}^2\sigma}{\mathrm{d}x\,\mathrm{d}y}\right|^{a}_{\mathrm{CC}}(e^{\pm}) \Bigg/ \left.\frac{\mathrm{d}^2\sigma}{\mathrm{d}x\,\mathrm{d}y}\right|^{\mathrm{Born}}_{\mathrm{CC}}(e^{\pm}) - 1, \tag{27}$$

where in $\mathrm{d}^2\sigma/\mathrm{d}x\,\mathrm{d}y|^a_{\mathrm{CC}}$ are included the leptonic, quarkonic or interference contributions only as denoted by the index $a = \ell, \mathrm{q}, \mathrm{i}$. δ^a_{CC} do not contain the bulk of weak corrections but only certain terms containing logarithms of s, t, and u which can become large at small values of x, y or $1-y$ and are compensated by corresponding contributions from the bremsstrahlung [2]. In order to compare our results with those of ref. [2] we have chosen the now obsolete values for the weak boson masses $M_{\mathrm{W}} = 82.0$ GeV and $M_{\mathrm{Z}} = 93.0$ GeV besides $m_{\mathrm{u}} = m_{\mathrm{d}} = 30$ MeV,

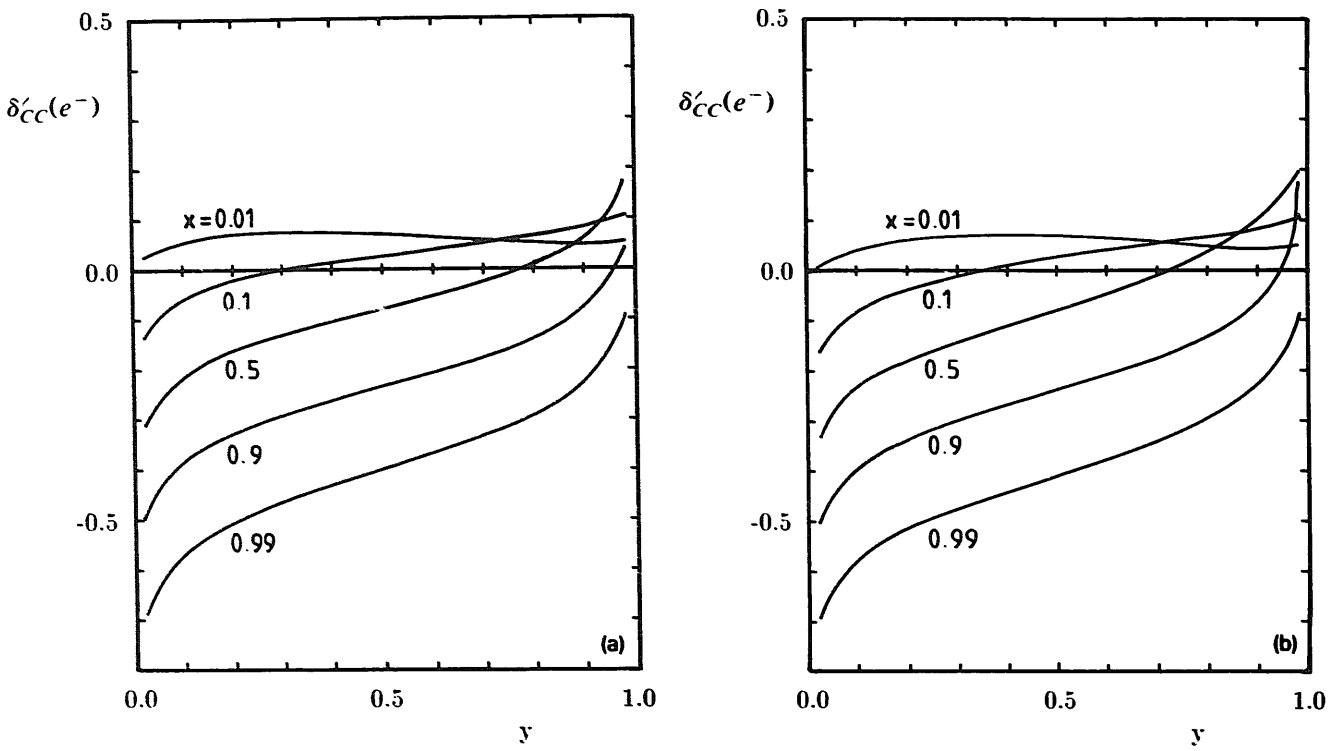

Fig. 5. Leptonic corrections δ'_{CC} for electron and positron scattering.

$m_t = 60$ GeV, $M_H = 100$ GeV. The parametrizations of the quark distributions are taken from ref. [17]. The results for the individual parts do not contain exponentiation. They agree perfectly well with those of ref. [2]. The similarity of the results as compared to those for the neutral current case with pure Z exchange [6] shows that the separation in eq. (8) was indeed sensible.

The quarkonic corrections $\delta^q_{CC}(e^\pm)$ yet contain the quark mass logarithms that should be absorbed into the quark distribution functions. The results of fig. 6 should therefore not be included in the derivation of corrections for physical observables as they stand. We present them here for the reason to compare our results with those of ref. [2]. The only physically observable feature of this part of the corrections is the Q^2 dependence of $\delta^q_{CC}(e^\pm)$ visible in the figures. In ref. [6] it has already been explained how the quarkonic corrections should be treated and we do not repeat this discussion here.

We want to point out that the corrections would have looked differently if the kinematical variables x and Q^2 would have been defined by the momentum of the outgoing quark rather than by that of the unobserved neutrino, e.g. with the help of the Jaquet–Blondel formula [10]. In the first case, the phase space integration is performed with fixed q', whereas in the latter case p' would remain fixed. The exchange of these two momenta amounts to an exchange of the invariants t and u. This enters into the formulas for the phase space limits which are the most

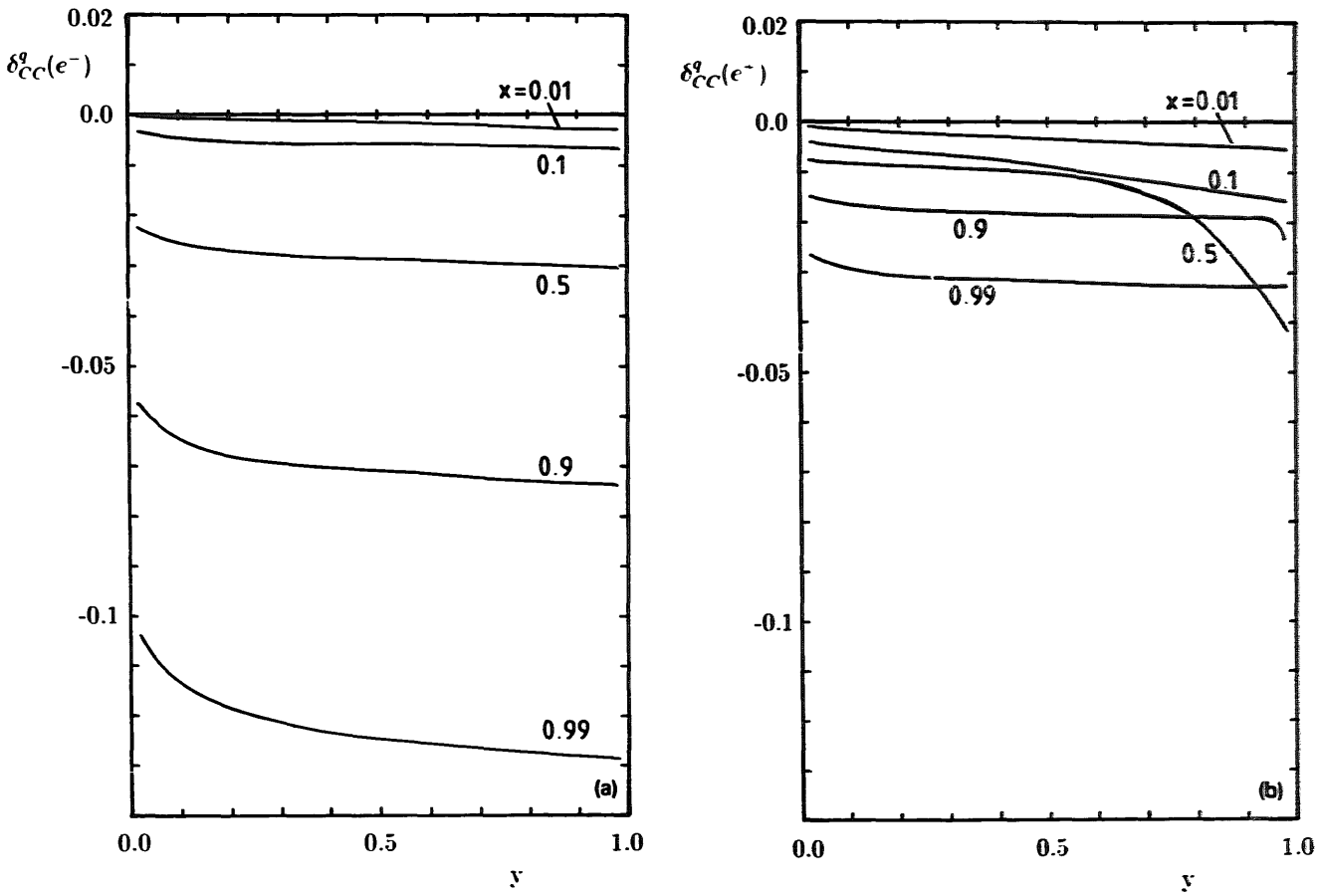

Fig. 6. Quarkonic corrections δ^q_{CC} for electron and positron scattering.

important sources of the peculiar raise of the leptonic corrections with y. This main feature can already be understood in the calculation of the leptonic corrections in the collinear approximation. There the initial state leptonic corrections are described by

$$\left.\frac{d^2\sigma}{dx\,dy}\right|^{in,\prime} = \frac{\alpha}{2\pi}\ln\frac{Q^2}{m_e^2}\left\{\int_{z_{min}}^1 dz\,\frac{1+z^2}{1-z}(\hat{\sigma}(z)-\hat{\sigma}(1)) + S(z_{min})\hat{\sigma}(1)\right\} \quad (28)$$

with

$$S(z) = 2\ln(1-z) + z + \tfrac{1}{2}z^2. \quad (29)$$

The integral contains the well-known Altarelli–Parisi splitting function that describes the emission of an energy fraction $1-z$ by collinear photons. $\hat{\sigma}(z)$ is the lowest order cross section where the momentum of the initial radiating lepton is rescaled by z and $S(z_{min})$ contains soft and virtual contributions.

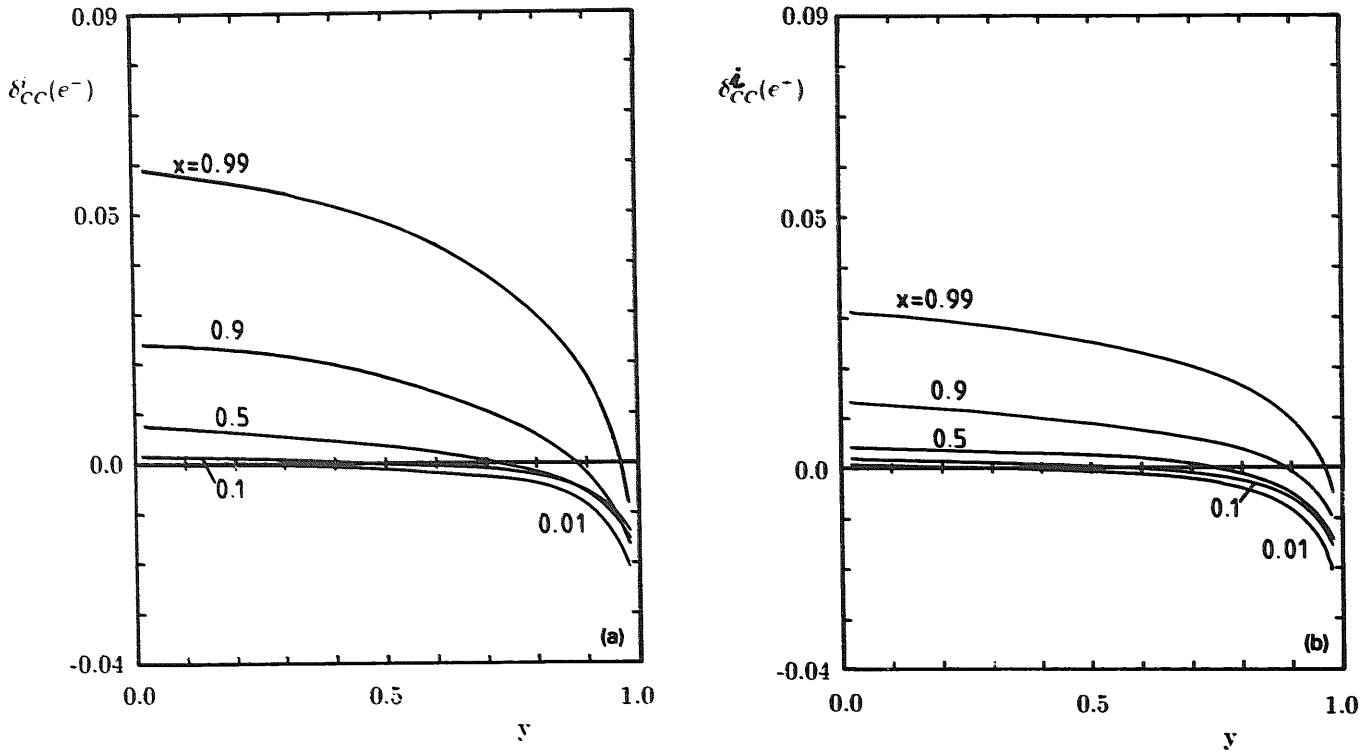

Fig. 7. Contribution of the interference of leptonic and quarkonic radiation $\delta^{\text{int}}_{\text{CC}}$ for electron and positron scattering.

If one calculates the range of integration of the energy variable z one would find for a fixed neutrino momentum $z_{\min} = (1-y)/(1-xy)$ whereas in the second case where the final quark momentum is fixed it was $z_{\min} = y/(1-x(1-y))$. Consequently the plots would look essentially as following from exchanging $y \leftrightarrow 1-y$ [18].

Finally in fig. 8 the results for the complete $O(\alpha)$ electroweak corrections are shown. This figure contains also the results of the exponentiated version of the cross section (24). The main effect of the soft photon exponentiation is the raising of the curves at small y and large x to less negative values, but there is also a visible effect for small values of x. For small x and y the non-IR parts δ^f_{fin} become large and the second order contribution $\delta_{\text{YFS}}\delta^f_{\text{fin}}$ induced by the exponentiation leads to the lowering of the corrections.

6. Fixed M_{W} versus fixed G_μ

Next to the photonic corrections discussed above the most important $O(\alpha)$ contribution is the W self-energy Π^{W}. It amounts to about 15%. It is only logarithmically Q^2 dependent and does not differ much from its value at $Q^2 = 0$ which in turn dominates the $O(\alpha)$ correction Δr to the M_{W}–G_μ relation. Conse-

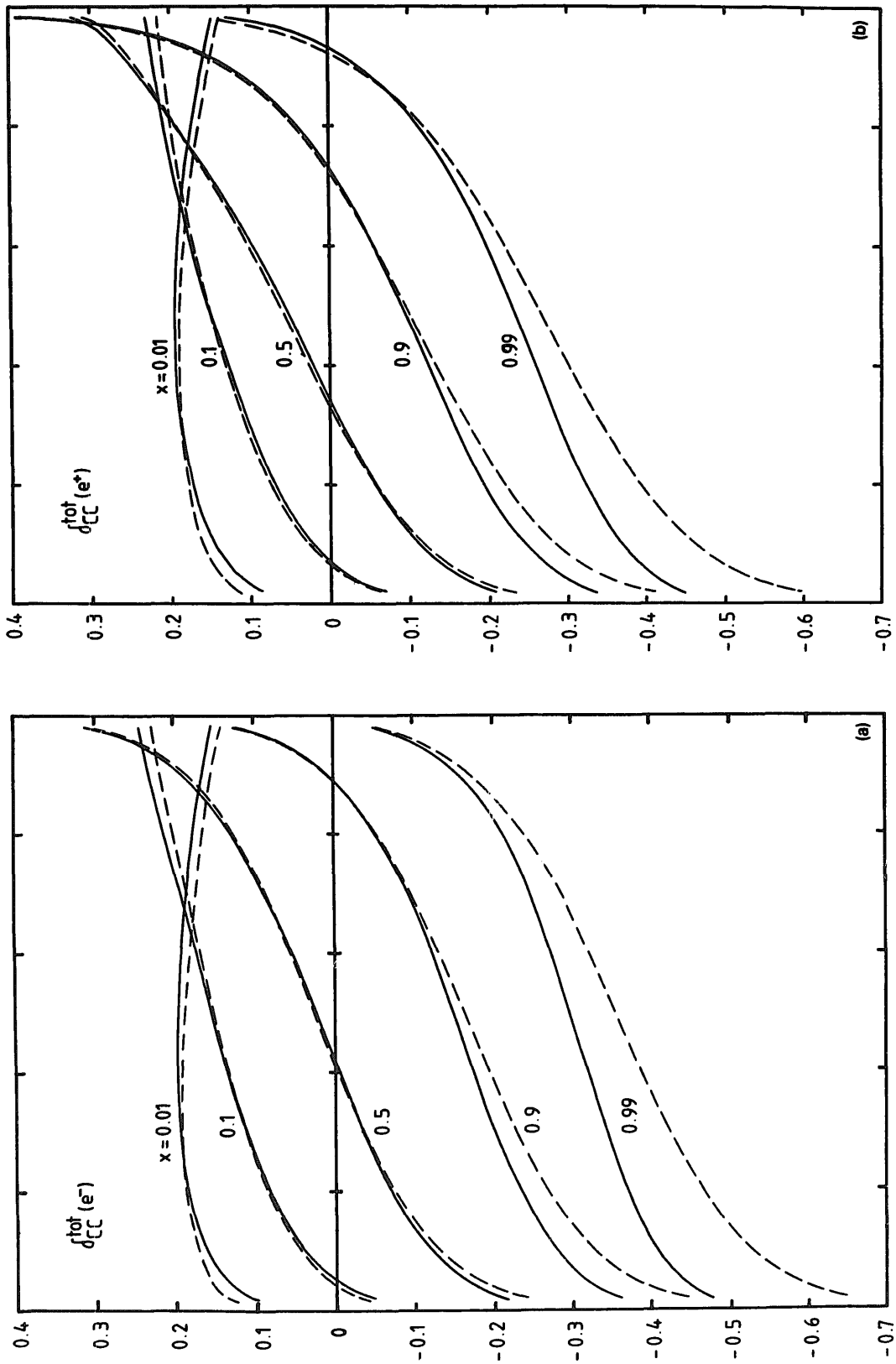

Fig. 8. Complete electroweak corrections to the charged current electron and positron scattering. The dashed curves show the $O(\alpha)$ predictions, the full lines include exponentiation of soft photonic corrections. ($M_W = 80.0$ GeV, $M_Z = 91.1$ GeV, $m_l = 80$ GeV, light quark masses: $m_q = 41$ MeV, parton distributions from ref. [17]).

quently, part of the corrections is already included in the Born expression, if that value of M_W is inserted that is derived from M_Z and G_μ using the radiatively corrected relation (5). This "improved" Born expression of the MOMS reads

$$\left.\frac{d^2\sigma}{dx\,dy}\right|_{CC}^{\text{improved Born}} = \frac{G_\mu^2 M_W^4 (1-\Delta r)^2}{\pi} \frac{xS}{(Q^2+M_W^2)^2}\{q+(1-y)^2\bar{q}\}. \quad (30)$$

The numerical results for δ_{CC}^{tot} are smaller by about 15% in this case.

The W self-energy receives a contribution from the top–bottom loop which rises quadratically with increasing m_t. In discussing the top mass dependence it becomes important to state precisely what kind of input parameters are used because via Δr the M_W–G_μ relation contains corrections of the same kind. In the on-mass-shell scheme with fixed M_W there is only the direct W self-energy correction which introduces an m_t dependence:

$$\left.\frac{d^2\sigma}{dx\,dy}\right|_{CC}^{OMS} = \left.\frac{d^2\sigma}{dx\,dy}\right|_{CC}^{Born} (1-2\Pi^W+\delta^{rest})$$

$$\simeq \left.\frac{d^2\sigma}{dx\,dy}\right|_{CC}^{Born} (1+2\Delta r+\delta^{rest}). \quad (31)$$

All other (m_t independent) contributions are contained in δ^{rest}. In order to illustrate the situation we show predictions for the NC/CC ratio [19]*

$$R_- = \frac{d\sigma(e^-\to e^-X)}{d\sigma(e^-\to \nu_e X)} \quad (32)$$

in fig. 9 for two different points in the (x, y) plane (corresponding to $Q^2 = 10^3$ GeV^2 in fig. 9a and $Q^2 = 10^4$ GeV^2 in fig. 9b). These figures contain also the band of variation resulting from the present experimental uncertainty of M_W of ± 0.6 GeV. The result for R_- in the OMS is rising by about 10% of its value at $m_t = 50$ GeV if m_t is increased to 250 GeV.

In the modified on-mass-shell scheme, where G_μ is used as input, M_W itself depends on m_t. Eq. (5) can be solved for M_W if the slight M_W dependence of Δr

* The m_t dependence of the neutral current cross section is obviously not important for this discussion. In fact, the neutral current is dominated for not too large values of Q^2 by the γ exchange which does not receive corrections proportional to m_t^2.

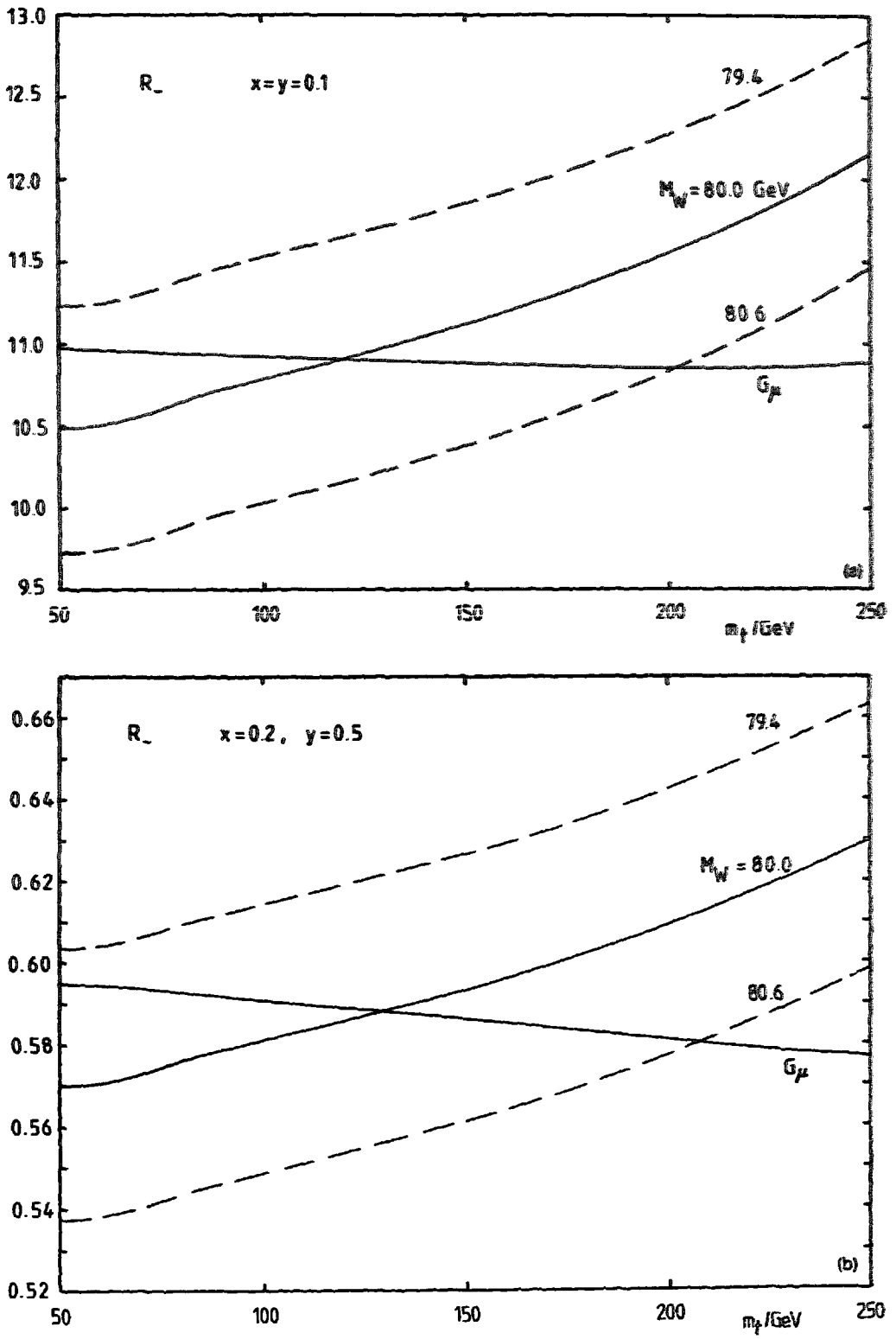

Fig. 9. (a) Top mass dependence of the NC/CC ratio R_- for electron scattering at $x = y = 0.1$ ($Q^2 = 10^3$ GeV^2). $M_H = 100$ GeV. (b) Top mass dependence of the NC/CC ratio R_- for electron scattering at $x = 0.2$, $y = 0.5$ ($Q^2 = 10^4$ GeV^2). $M_H = 100$ GeV.

is neglected as

$$M_W^2 = \tfrac{1}{2} M_Z^2 \left(1 + \sqrt{1 - \frac{4\pi\alpha}{\sqrt{2} G_\mu M_Z^2 (1 - \Delta r)}} \right). \tag{33}$$

Because Δr is of order α one can expand eq. (33) in powers of Δr. To first order one finds

$$M_W^2(G_\mu, M_Z, \Delta r) = M_W^2(G_\mu, M_Z, 0) \left(1 - \frac{s_W^2}{2c_W^2 - 1} \Delta r \right). \tag{34}$$

With this one finds for the cross section in the MOMS

$$\left. \frac{d^2\sigma}{dx\,dy} \right|_{CC}^{MOMS} = \left. \frac{d^2\sigma}{dx\,dy} \right|_{CC}^{Born} \left(1 - 2\Delta r - 2\Pi^W - 2\frac{s_W^2}{2c_W^2 - 1} \Delta r + \delta^{rest} \right)$$

$$\simeq \left. \frac{d^2\sigma}{dx\,dy} \right|_{CC}^{Born} \left(1 - 2\frac{s_W^2}{2c_W^2 - 1} \Delta r + \delta^{rest} \right). \tag{35}$$

The coefficient of Δr is here about -0.80 for $s_W^2 = 0.221$ whereas in the corresponding expression (31) of the OMS it was $+2$.

The m_t dependence of M_W is the main source of the m_t dependence of R_- in the MOMS. However, it is visible only for larger values of Q^2 (as in fig. 9b). For low Q^2 one can approximate $M_W^4/(Q^2 + M_W^2)^2$ by 1: the Fermi model is still a good approximation and one remains with the μ decay constant that determines the magnitude of the charged current cross section. Indeed, for $Q^2 = 10^3$ GeV^2 the m_t dependence of R_- shown in fig. 9a is completely negligible whereas for $Q^2 = 10^4$ GeV^2 the top mass dependence in the MOMS although rather flat leads to a decrease of R_- by about 3% if m_t is increased from 50 GeV to $m_t = 250$ GeV. It is determined by the m_t dependence of M_W^4 in the numerator of the charged current cross section.

We want to point out that the OMS and the MOMS are not two different renormalization schemes in the usual sense. In both schemes, the generation of counter-terms and the definition of renormalization constants are identical. The OMS and the MOMS rather differ in the way the parameters are fixed by experimental inputs. When comparing results for R_- (at given values for M_Z, m_t, M_H, etc.) for fixed G_μ with results for R_- at fixed M_W one is actually comparing results calculated at two different points in the parameter space, except if one chooses exactly that value for M_W which results from the solution of eq. (5).

TABLE 1
NC/CC ratio R_- for electron scattering at $x = y = 0.1$ ($Q^2 = 10^3$ GeV^2). $m_t = 100$ GeV.

M_H (GeV)	R_-^{OMS} $M_W = 79.4$ GeV	R_-^{OMS} $M_W = 80.0$ GeV	R_-^{OMS} $M_W = 80.6$ GeV	R_-^{MOMS}
10	11.62	10.83	10.04	10.91
100	11.53	10.78	10.03	10.93
1000	11.35	10.60	9.86	10.95

We should briefly mention that there is also a Higgs mass dependence in $R_\pm$. In tables 1 and 2 results are given for $m_t = 100$ GeV. It follows from the given numbers that the dependence on M_H is small as compared to that on M_W or m_t.

We have shown explicit results only for the cross section ratio R_- for electron scattering but the discussion applies equally well to positron scattering.

Finally, we want to mention that the polarization and charge asymmetries in the neutral current reaction, e.g.

$$A_\pm = \frac{d\sigma(e_L^\pm) - d\sigma(e_R^\pm)}{d\sigma(e_L^\pm) + d\sigma(e_R^\pm)} \tag{36}$$

are probably better suited for a possible determination of m_t limits in deep inelastic scattering via radiative corrections. $A_\pm$ is also a ratio of a purely weak part (the difference of cross sections for left-handed and right-handed leptons) and a sum of cross sections which is determined essentially by the γ exchange. In this case the Z self-energy Π^Z appears as a genuine contribution to the radiative corrections instead of the W self-energy. The m_t dependent terms in Π^Z do not cancel completely against the factor $1 - \Delta r$ if G_μ is used as input but the coefficients of m_t^2 in Δr and in Π^Z do not differ much and also in this case one finds a weak dependence in the MOMS as compared to a much stronger m_t dependence in the OMS. With fixed G_μ the change of A_- is of order O(10%) if m_t is varied in the range between 50 and 250 GeV. In the OMS, however, one

TABLE 2
NC/CC ratio R_- for electron scattering at $x = 0.2$, $y = 0.5$ ($Q^2 = 10^4$ GeV^2). $m_t = 100$ GeV.

M_H (GeV)	R_-^{OMS} $M_W = 79.4$ GeV	R_-^{OMS} $M_W = 80.0$ GeV	R_-^{OMS} $M_W = 80.6$ GeV	R_-^{MOMS}
10	0.618	0.584	0.551	0.589
100	0.615	0.581	0.549	0.591
1000	0.608	0.575	0.543	0.594

does not gain much because the experimental uncertainty of M_W does not allow us to derive stringent limits on m_t.

7. Conclusions

We have presented results of a complete calculation of the $O(\alpha)$ electroweak radiative corrections to charged-current deep inelastic lepton–proton scattering. The corrections can be large of the order of O(20%) for small x and negative of the order of $O(-40\%)$ for large x and small y and are therefore nonnegligible. The comparison with a similar calculation by Bardin et al. has shown agreement below the 1% level. This is satisfactory if one bears in mind that the charged current scattering at HERA will probably not be an experiment that reaches that precision.

It has been shown that soft photon exponentiation leads to additional corrections of a few percent. Only for small y this multiple photon effect comes close to the expected experimental accuracy. Higher order contributions to the weak corrections have not been calculated but estimations in ref. [20] show that for the precision that could be reached at HERA they will certainly be negligible.

We have applied a Monte Carlo integration technique for the evaluation of the hard bremsstrahlung contribution. By a suitable choice of variables we could make the integrand well behaved. This method will be used in the near future in the development of an event generator that simulates charged current scattering at HERA including radiative effects.

The discussion of the 1-loop corrections was done with special emphasis on the top quark mass dependence of the W self-energy. It was shown that the sensitivity on m_t is large if a fixed input value for the W boson mass is used. But the experimental uncertainty on M_W prevents us from using the m_t dependence in this case to derive limits on the top quark mass. Instead of this one should use a formulation of the theory in terms of the μ decay constant G_μ. Then the allowed range for m_t could be restricted to ± 50 GeV if the NC/CC cross section ratio could be measured with a precision of better than $\pm 1\%$ at not too small Q^2.

I would like to thank M. Böhm, J. Blümlein, W. Hollik, G. Kramer, T. Riemann, and G. Schuler for helpful discussions. I am also grateful to G. Hummel for many enlightening conversations.

References

[1] D.Yu. Bardin, C. Burdik, P.Ch. Christova and T. Riemann, Dubna preprint E2-87-595, E2-88-682; Z. Phys. C42 (1989) 679
[2] D.Yu. Bardin, C. Burdik, P.Ch. Christova and T. Riemann, Z. Phys. C44 (1989) 149
[3] M. Böhm and H. Spiesberger, Nucl. Phys. B294 (1987) 1081
[4] M. Böhm and H. Spiesberger, Nucl. Phys. B304 (1987) 749

[5] W. Hollik, CERN-TH.5547/89 (1989)
[6] H. Spiesberger, DESY 89-175 (1989)
[7] J. Blümlein, Int. Warsaw Symp. on High energy physics, Kazimierz, Poland 1989, ed. Z. Adjuk and S. Pokorski; Berlin-Zeuthen preprint PHE 89-12 (1989)
[8] A. Kwiatkowski, H.-J. Möhring and H. Spiesberger, in preparation
[9] D.R. Yennie, S.C. Frautschi and H. Suura, Ann. Phys. (NY) 13 (1961) 379
[10] A. Blondel and F. Jaquet, ECFA Report, Proc. of the Study of an ep facility for Europe, DESY 79/48 (1979), p. 393
[11] R.D. Peccei, ed., Proc. of the HERA Workshop, Hamburg 1987, Vol. 2, p. 577
[12] M. Böhm and W. Hollik, H. Spiesberger, Fortschr. Phys. 34 (1986) 687
[13] A. Sirlin, Phys. Rev. D22 (1980) 971
[14] A. de Rújula, R. Petronzio and A. Savoy-Navarro, Nucl. Phys. B154 (1979) 394
[15] S. de Jong and J. Vermaseren, AXO user manual (NIKHEF-H, Amsterdam, 1987)
[16] J. Kripfganz, H.-J. Möhring and H. Spiesberger, in preparation
[17] D.W. Duke and J.F. Owens, Phys. Rev. D30 (1984) 49
[18] J. Kripfganz and H.-J. Möhring, Z. Phys. C38 (1988) 653
[19] J. Blümlein, M. Klein and T. Riemann, *in* Proc. of the HERA Workshop, Hamburg 1987, ed. R.D. Peccei, Vol. 2, p. 687
[20] F. Jegerlehner, Z. Phys. C32 (1986) 425;
W. Hollik and H.-J. Timme, Z. Phys. C33 (1986) 125